Rheological Modeling, Spectroscopic and Physicochemical Characterization of *Raphia hookeri* (*RH*) Gum Exudate

Nnabuk Okon EDDY[1,3,*], Inemesit UDOFIA[1], Stephen Eyije ABECHI[1], Edward OKEY[2] and Anduang ODIONGENYI[3]

[1]*Department of Chemistry, Ahmadu Bello University, Zaria Kaduna, Nigeria*
[2]*Department of Biological Sciences, Akwa Ibom State University, Akwa Ibom, Nigeria*
[3]*Department of Chemistry, Akwa Ibom State University, Akwa Ibom, Nigeria*

([*]**Corresponding author's e-mail: nabukeddy@yahoo.com, abeshus@yahoo.com**)

Abstract

Raphia hookeri (*RH*) gum exudate has been analysed for physical (colour, odour, taste, pH, salinity, turbidity), chemical (solubility in some solvents, proximate/elemental composition, vitamin composition, phytochemicals and anti-nutrients) and spectroscopic (wavelength of maximum absorption, GCMS, FTIR and SEM) properties. The results obtained from the study revealed that *RH* gum has the potential for utilization as an emulsifier, a food additive and as a pharmaceutical excipient. Rheological modeling on the gum revealed that the average intrinsic value of the gum, (deduced from Huggins, Kraemer, Tanglerpaibul and Rao models) is approximately 3.0 dl/g. The calculated values of Huggins and Kraemer constants revealed the existence of molecular association in the gum. The gum is found to possess unique rheological properties including absence of degradation/conformational changes, existent of intra and inter molecular interactions, adoption of random coil model and absent of coil overlap transition. *RH* gum is a shear thinning, non- Newtonian gum with pseudo-plastic behavior. The calculated thermodynamic parameters were comparable to those reported for some food gums.

Keywords: *Raphia hookeri* gum, physicochemical analysis, rheological modeling, food additives, pharmaceutical excipient

Introduction

Most plant gums have been found to be useful in food, pharmaceutical, metallurgical, cosmetic, beverage and other industries [1-5]. It has been found that the various utilizations that can be harnessed from gums depend on their physiochemical, rheological and surface properties [6]. For example, food and pharmaceutical gums must not be toxic and their composition must conform to those expected for such purposes.

In view of the numerous advantages of gums, chemical properties of several gums have been studied. These include those of *Albizia* species gums [7], *Acacia Senegal* gum [8,9], *Cissuspopulnea* [10], *Ferula gumosa* gum [11], *Anogeissusleiocarpus* [12] and others. Similarly, studies on the rheological properties of gum Arabic, methyl cellulose and pectin have been reported [13]; Rheological properties of *Albizia lebeck* gum exudates [14], tarmarind seed gum [15], peach tree gum [16] and Guar gum [17] have also been reported.

Raphia Hookeri gum exudates are naturally occurring polysaccharides containing hexuronic acid units as salts and a number of neutral monosaccharide units which are often esterified into branched structures. The source of the exudates is the *Raphia* palm tree and the gum can be produced by deliberately injuring the fibro vascular tissues of the apex, (the inflorescence) of the *Raphia* palm [1,18].

Some studies have been reported on the proximate composition of *Raphia hookeri* gum [1,5] and the gum was reported to be a good source of minerals and vitamins. However, to the best of our knowledge, no work has reported detailed physicochemical, surface and rheological compositions of *Raphia hookeri* gum exudates. The present study is therefore aimed at investigating the physical, chemical, elemental, functional group, rheological and surface properties of *Raphia hookeri* gum exudates.

Materials and methods

Collection and purification of samples

Crude *RH* gum was obtained as exudates from Raphia palm trees grown in Ikot Ekpene in Akwa Ibom State, Nigeria. The procedure adapted for the purification of the gum was as follows; the gum sample was dried in an oven at 40 °C for 2 h and ground with a blender. It was hydrated twice using chloroform water (in a ratio of 70:30 for water:chloroform) for 5 days with intermittent stirring to ensure complete dissolution of the gum and then strained through a 75 μm sieve to obtain a particulate free slurry which was allowed to sediment. Thereafter, the gum was precipitated from the slurry using absolute ethanol, filtered and defatted with diethyl ether. The precipitate was dried at 40 °C for 48 h. The dried flakes were pulverized using a blender and stored in an air tight container.

Physiochemical analysis

In order to characterize the gums, it was subjected to the following physiochemical tests.

Determination of percentage yield of the purified gums

The dried, precipitated and purified gum(s) obtained from the crude dried exudates were weighed and the percentage yields were expressed in percentage using the weight of the crude gum(s), as the denominator.

Determination of percentage moisture sorption

In order to determine the water sorption capacity of the gum, dried evaporating dishes were weighed and 2.0 g of the gum sample was weighed into the dish. The final weight of the dishes were noted and placed over water in desiccators. After 5 days, the dish was transferred to other desiccators over activated silica gel (desiccant) for another 5 days. The percentage sorption was calculated by difference in weight.

Determination of solubility

The solubility of the gum was determined in cold and hot distilled water, acetone, chloroform and ethanol. A 1.0 g sample of the gum was added to 50 ml of each of the solvents and left overnight. Twenty five ml of the clear supernatants were placed in small pre-weighted evaporating dishes and heated to dryness over a digital thermostatic water bath. The weights of the residues with reference to the volume of the solutions were determined using a digital top loading balance (Model XP-3000) and expressed as the percentage solubility of the gums in the solvents.

Determination of vitamins, phytochemicals and anti-nutrients

The phytochemical constituents of the gum (alkaloid, saponins, phenols and flavonoids) and its vitamins contents were determined by the methods reported by Okwu and Nnamdi [5]. Anti-nutritional contents of the gum were determined using the methods reported by Akpabio *et al*. [1].

Determination of concentration of metals

Concentrations of metals were determined using a Perkin Elmer atomic absorption spectrophotometer. A calibration curve for each metal was prepared and the concentration of the metal in the analyte was estimated by extrapolation.

Determination of nitrogen and protein content
The nitrogen content of the gum was determined using the Kjedahl method and the protein content was estimated by multiplying the nitrogen content by a conversion factor of 6.25.

Determination of pH
This was done by shaking a 1 % w/v dispersion of the sample in distilled and deionized water (pH = 6.98) for 5 min and the pH was determined using a pre-calibrated Oaklon pH meter (Model 1100).

Determination of refractive index of the gums
An Eloptron refractometer was used to determine the refractive index of the gum.

Determination of moisture content
The moisture content of the sample was determined by the oven drying method described in AOAC [19].

Determination of ash content
The ash content of the sample was determined using the method recommended by AOAC [19].

Determination of crude lipid content
The lipid content was determined using the method recommended by AOAC [19].

Determination of crude fibre
The method described by AOAC [19] was adopted for the determination of the fibre content of the sample.

Determination of carbohydrate (by method of difference)
The total carbohydrate content was determined by difference. The sum of the percentage moisture, ash, crude lipid, crude protein, and crude fibre was subtracted from 100 [20]. The total carbohydrate in the sample was calculated using the following equation;

% Total carbohydrate = 100 - (Moisture + Ash + Fat + Protein + Fibre) %.

Determination of salinity and turbidity
The salinity and turbidity of the gum were determined using salinity and turbidity meters respectively.

GC-MS analysis
The analysis was carried out on a GC clarus 500 Perkin Elmer system comprising a AOC-20i Autosampler and Gas Chromatograph interfaced to a Mass Spectrometer (GC-MS). The instrument employed the following conditions: a column Elite-1 fused silica capillary column (30 × 0.25 mm ID × 1 μmdf, composed of 100 % Dimethyl polydioxane), operating in electron impact mode at 70 eV. Helium (99.99 %) was used as the carrier gas at a constant flow of 1 ml/min and an injection volume of 0.5 μL was employed (split ratio of 10:1) with an injector temperature of 250 °C; an ion-source temperature of 280 °C. The oven temperature was programmed from 110 °C (isothermal for 2 min), with an increase of 10 °C/min, to 200 °C, then 5 °C/min to 280 °C, ending with a 9 min isothermal at 280 °C. Mass spectra were taken at 70 eV; a scan interval of 0.5 s and fragments from 40 to 450 Da. The total GC running time was 36 min.

Interpretation of GC-MS spectrum
Interpretation of the mass spectrum GC-MS was conducted using the database of National Institute Standard and Technology (NIST), which has more than 62,000 patterns. The spectrum of the unknown

component was compared with the spectrum of the known components stored in the NIST library. The name, molecular weight and structure of the components of the test materials were ascertained. Concentrations of the identified compounds were determined through area and height normalization.

Viscosity measurements

The intrinsic viscosity of the *RH* gum sample was determined in distilled water using a Cannon Ubbelohde capillary viscometer (Cannon Instruments, model I-71) which was immersed in a precision water bath maintained at 25 °C. The apparent viscosity of the mucilage was measured using a digital Brookfield DV I prime viscometer while shear rate was measured using a Schott Iberica, S.A 18549 rotational viscometer.

Scanning electron microscopy examinations

The morphological features of the gums were studied with a JSM-5600 LV scanning electron microscope (SEM) of JEOL, Tokyo, Japan. The dried sample was mounted on a metal stub and sputtered with gold in order to make the sample conductive, and the images were taken at an accelerating voltage of 10 kV.

FTIR analysis

FTIR analysis of the gum was carried out using a Scimadzu FTIR-8400S Fourier transform infra-red spectrophotometer. The sample was prepared in KBr and the analysis was carried out by scanning the sample through a wave number range of 400 to 4000 cm^{-1}.

Results and discussions

Physicochemical composition

Figure 1 shows photographs of crude and purified samples of the gum while **Table 1** presents physicochemical constituents of *RH* gum exudates. After purification of the crude gum samples, yield of 86.60 % was obtained, which is relatively high.

Purified   **Crude**

Figure 1 Photograph of crude and purified samples of *RH* gum exudates.

RH gum is milky yellow in colour and has a sour taste, which complements its mildly acidic nature (pH = 4.88). The conductivity of the gum (218.30 µS/cm) is comparable to those reported for ionic macro molecules [21]. One of the major characteristics of the ionic compounds is that they are soluble in water and in solvents that have a high dielectric constant unlike non-ionic compounds, which are insoluble in

water but soluble in organic solvent. From the results obtained, it is evidence that *RH* gum is soluble in water but insoluble in ethanol, acetone, and chloroform, indicating that the gum is ionic. The solubility of the gum in water was found to increase with an increase in temperature, which suggests that the degree of solute- solvent interaction increases as the temperature increases. Although RH gum is ionic, the measured salinity (0.4) was relatively low implying that the conductivity of the gum may not be a function of its chloride content but due to adsorption of charges. The gum is highly turbid; therefore it has the potential of scattering light and may serve as a good emulsion stabilizer [22]. The maximum adsorption for the studied gum was at 310 nm.

Table 1 present the proximate composition of *RH* gum including its carbohydrate, protein, moisture, vitamins, ash, fibre, fat and oil contents. It is significant to note that the *RH* gum has a high concentration of carbohydrates, which can be attributed to the presence of several forms of polysaccharides. Nitrogen (0.49 %) and protein (3.06 %) content of the gum is relatively low compared to the value (16.6 %) reported by Okwu and Nnamdi [5]. The difference may be due to losses during processing. The low protein content of the gum, coupled with the absence of fibre also confirms that the gum has excellent emulsifying properties [22].

The ash content of the gum (0.47 %) is lower than that (1.72 %) reported by Okwu and Nnamdi [5] and is also lower than those reported for some plant gums including *Acacia senegal* gum (3.77 %) [23] and *Anogeissus leiocarpus* gum of various species (2.2 to 4.5 %) [12]. The difference may also be due to processing. Moisture content of the gum was measured as 12.00 % while its lipid content was 1.00 %. These values compare favourably with those obtained by Okwu and Nnamdi [5] for *Raphia hookeri* gum exudates. The low lipid content of the gum also confirms that *RH* gum is a good emulsifying agent [22]. Mean concentrations of essential vitamins (including ascorbic acid, niacin, riboflavin and thiamine) in *RH* gum are closely comparable to those obtained by Okwu and Nnamdi for *RH* gum exudates [5].

Vitamins are essential in human nutrition. Ascorbic acid for instance, is needed for the formation of intracellular substances such as collagen in the body. According to Okwu and Nnamdi [5], deficiency of any of the vitamins can cause widespread clinical symptoms. From the results of the present study, the vitamins composition of *RH* gum was found to be relatively low; nevertheless, the values are comparable to those reported for nutrient rich food.

RH gum was found to be rich in essential elements, notably Ca (11.663 ppm) and Fe (1.039 ppm), relatively rich in trace elements, Zn (1.073 ppm), Mn (2.676 ppm), Cu (0.043 ppm) but exhibited very low concentrations (below permissible limits) of toxic heavy metals, Cd = −0.003 ppm; Ni = 0.115 ppm, Co = 0.005; Pb = 0.0074 ppm and Cr = 0.003 ppm. *RH* gum may therefore be useful in food and pharmaceutical industries. In order to further ascertain the level of toxicity of *RH* gum, anti-nutrient composition of the gum was also determined and the results obtained are presented in Table 1. Oxalate, hydrogen cyanide and phytic acid are the major anti-nutrients in most plant products. Mean concentration of hydrogen cyanide (2.30 mg/100 g) in the gum sample was below the lethal level of 35 mg/100g of the body weight and are comparable to values reported for most food materials [1]. However, this value is lower than that reported by Akpabio *et al*. [1] for *RH* gum. The variation may be due to the utilization of a processed sample in this study. Concentrations of soluble and total oxalates in the gum were also comparable to those reported for most food products and for the same reason, were lower than those reported in literature for *RH* gum [1,5]. Oxalate is capable of causing calcium deficiency in the body by complexing out calcium from the system. Phytic acid composition of the gum was also comparable to those reported for most food products and for reasons explained above, the value is lower than that reported earlier [1].

Mean concentrations of saponin, alkaloids, phenols and flavonoids in *RH* gum are comparable to those reported by Okwu and Nnamdi [5]. The presence of alkaloids and flavanoids in the exudates suggest that the gum has medicinal properties since the biological roles of alkaloids include protection against allergies, inflammation, free radicals scavenging, platelets aggregation, microbes, ulcers, hepatoxins, virus and tumors [24] while those of flavonoids is related to the inhibition of inflammation. Phenols have also been found to be useful in the protection of humans from oxidative damage through the blockage of enzymes that are responsible for inflammations.

Table 1 Physicochemical parameters of *RH* gum

Parameter	Result	Parameter (ppm)	Concentration
Colour	milky-yellow	Mn (ppm)	2.676
Odour	offensive	Fe (ppm)	1.039
Taste	sour	Zn(ppm)	1.075
pH (29.2 °C)	4.88	Mg (ppm)	0.646
Percentage yield (% w/v)	86.60	Ca (ppm)	11.663
Swelling capacity	12	Cu (ppm)	0.043
Solubility in cold water	8.4	Pb (ppm)	0.074
Solubility in hot water	8.9	Cd (ppm)	-0.003
Acetone	0.0	Ni (ppm)	0.115
Chloroform	0.0	Co (ppm)	0.005
Ethanol	0.0	Cr (ppm)	0.003
TDS (mg/l)	160.2	Ascorbic acid (mg/100g)	8.21
Conductivity (μs/cm)	218.5	Niacin (mg/100g)	3.23
Salinity (0/00)	0.4	Riboflavin (mg/100g)	0.81
Turbidity (FAU)	1098	Thiamine (mg/100g)	0.13
λ_{max}(nm)	310	Saponin (mg/100g)	2.98
Melting point (°C)	204 - 216	Alkaloids	0.52
Nitrogen (%)	0.49	Phenols	0.04
Protein (%)	3.06	Flavanoid	0.32
Ash content (%)	0.47	HCN (mg/100g)	2.30
Fat and Oil (%)	1.00	Soluble oxalate	7.86
Moisture content (%)	12.0	Total oxalate	16.42
Carbohydrate (%)	83.47	Phytic acid	6.87
Fibre content (%)	0.0		

GCMS study

Analytical data deduced from the GCMS spectrum of the *RH* gum are presented in **Table 2**. Chemical structures of likely compounds in the gum are shown in **Figure 2**. The results obtained indicated the presence of some alkenes; 1-undecene (2.04 %), 3-hexadecene (4.39 %) and 3-octadecene (5.80 %) in lines 1, 2 and 4. However, in line 3, 4.77 % of 3, 5-di-tert-butylphenol was identified under a retention time of 15.675 min. In lines 5 to 7, some aromatic compounds were identified. These included 2.48 % of 1-butylheptyl benzene, 1.65 % of 1-propyloctyl benzene and 2.70 % of 1-butyloctyl benzene. In line 8, 5.14 % of 1-docosene was isolated at a retention time of 20.375 min while carboxylic acids dominated lines 9 to 13 of the spectrum. The carboxylic acids included 8.09 % palmitic acid, 24.02 % n-hexadecanoic acid, 7.87 % 9, 12-octadecadienoic acid, 12.26 % 10-octadecenoic acid and 4.64 % n-octadecanoic acid. The acids were eluted at retention time values of 22.525, 23.433, 26.458, 26.458, 26.650 and 27.267 % respectively. Finally, in line 14, 14.15 % of nonanentrile was identified at a retention time of 27.558 min. Industrial applications and uses of the listed compounds are presented in the supporting information.
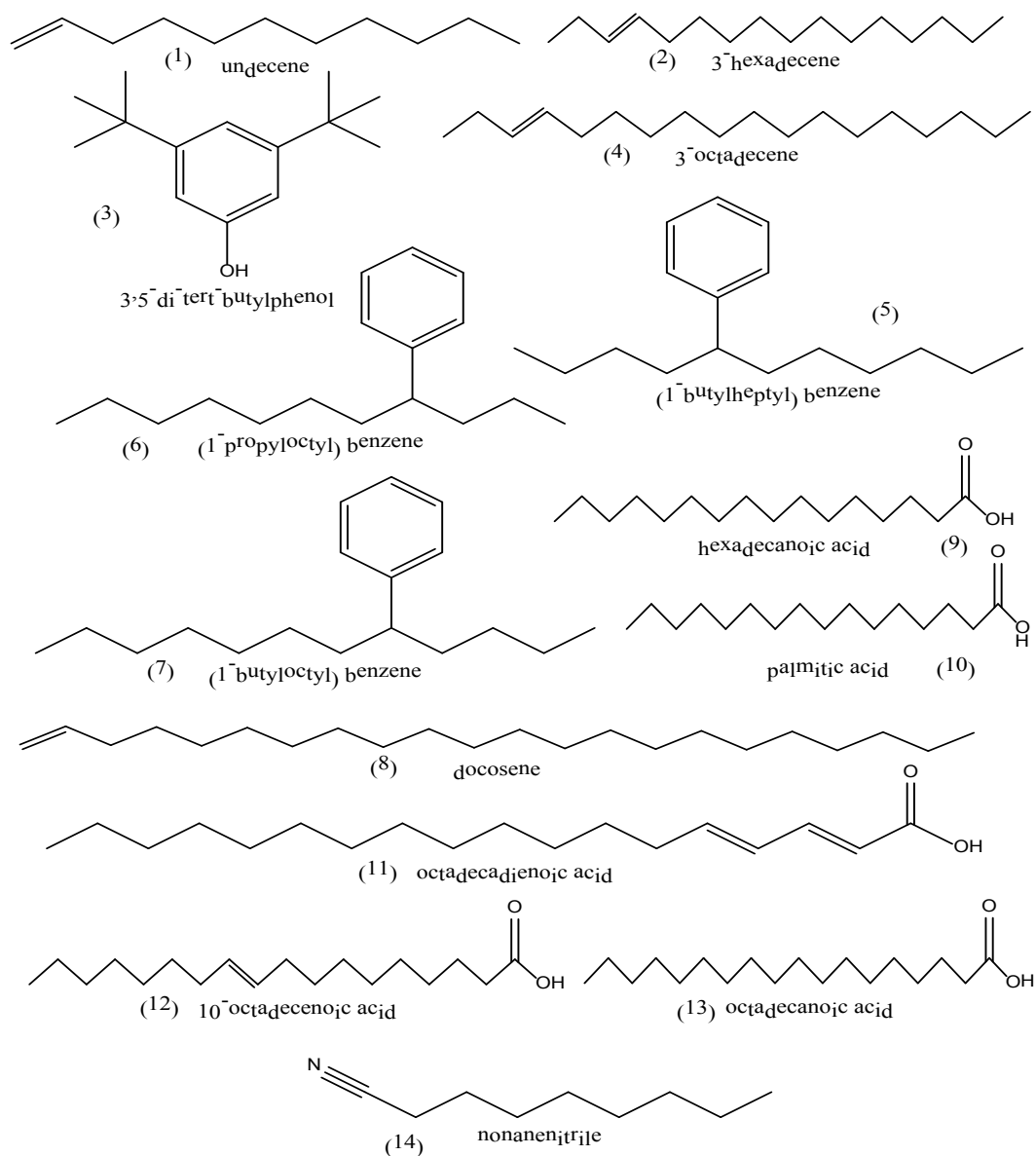
Figure 2 Chemical structures of compounds in *RH* gum.

Table 2 Analytical parameters deduced from GCMS spectrum of *RH* gum.

Line no	IUPAC name	Molecular formula	Molar mass (g/mol)	Retention time (m)	Concentration (%)
1	1-undecene	$C_{11}H_{22}$	154	9.658	2.04
2	3-hexadecene	$C_{16}H_{32}$	224	13.642	4.39
3	3,5-di-tert-butylphenol	$C_{14}H_{22}O$	206	15.675	4.77
4	3-octadecene	$C_{18}H_{36}$	252	17.192	5.80
5	1-butylheptyl benzene	$C_{17}H_{28}$	232	17.783	2.48
6	1-propyloctyl benzene	$C_{17}H_{28}$	232	17.958	1.65
7	1-butyloctyl bezene	$C_{18}H_{30}$	246	19.367	2.70
8	1-Docosene	$C_{22}H_{44}$	308	20.375	5.14
9	Palmitic acid	$C_{17}H_{34}O_2$	270	22.525	8.09
10	n-hexadecanoic acid	$C_{16}H_{32}O_2$	256	23.433	24.02
11	9,12-octadecadienoic acid	$C_{19}H_{34}O_2$	294	26.458	7.87
12	10-octadecenoic acid	$C_{19}H_{36}O_2$	296	26.650	12.26
13	n-octadecanoic acid	$C_{19}H_{38}O$	298	27.267	4.64
14	Nonanenitrile	$C_9H_{17}N$	139	27.558	14.15

FTIR study

Table 3 presents peaks and frequencies of IR absorption as well as functional functional groups deduced from the FTIR spectrum of RH gum. From the results obtained, it is evident that the gum displayed strong OH vibrations at 3449, 3342 cm^{-1}, CH stretches at 3177 and 3090 cm^{-1} [25]. A symmetric CH stretch was observed at 2939 cm^{-1} while the OH stretch due to the –COOH functional groups appeared at 1639 and 1430 cm^{-1} [25]. A C=O stretch due to an acetyl group was observed at 1246 cm^{-1} [26]. C-O stretches were found at 1139 and 1045 cm^{-1} while C-H bending vibrations due to alkynes were found at 797 and 629 cm^{-1}.

Table 3 Peak, frequency and assignment of FTIR absorption by *RH* gum.

Peak	Intensity	Area	Assignment
629	24.762	222.097	-C-H bend due to alkyne
797	29.994	45.194	-C-H bend due to alkyne
1045	19.765	148.108	C-O stretch
1139	22.086	52.442	C-O stretch
1246	23.559	66.288	-C=O stretch
1430	22.85	115.853	OH bending
1638	20.198	217.377	OH stretch
2939	21.701	352.038	C-H stretch
3090	20.381	85.709	C-H stretch
3177	19.444	68.808	C-H stretch
3342	18.503	131.808	OH stretch
3449	19.283	244.353	OH stretch

SEM study

Scanning electron microscopy (SEM) is utilized to record the images of a surface of materials/specimens at a desired position to obtain a topographic/morphological picture with better resolution and depth of focus compared to an ordinary optical microscope [27]. **Figure 3** shows the scanning electron micrographs of *RH* gum at 1.00, 3.00 and 5.00 K× magnifications.

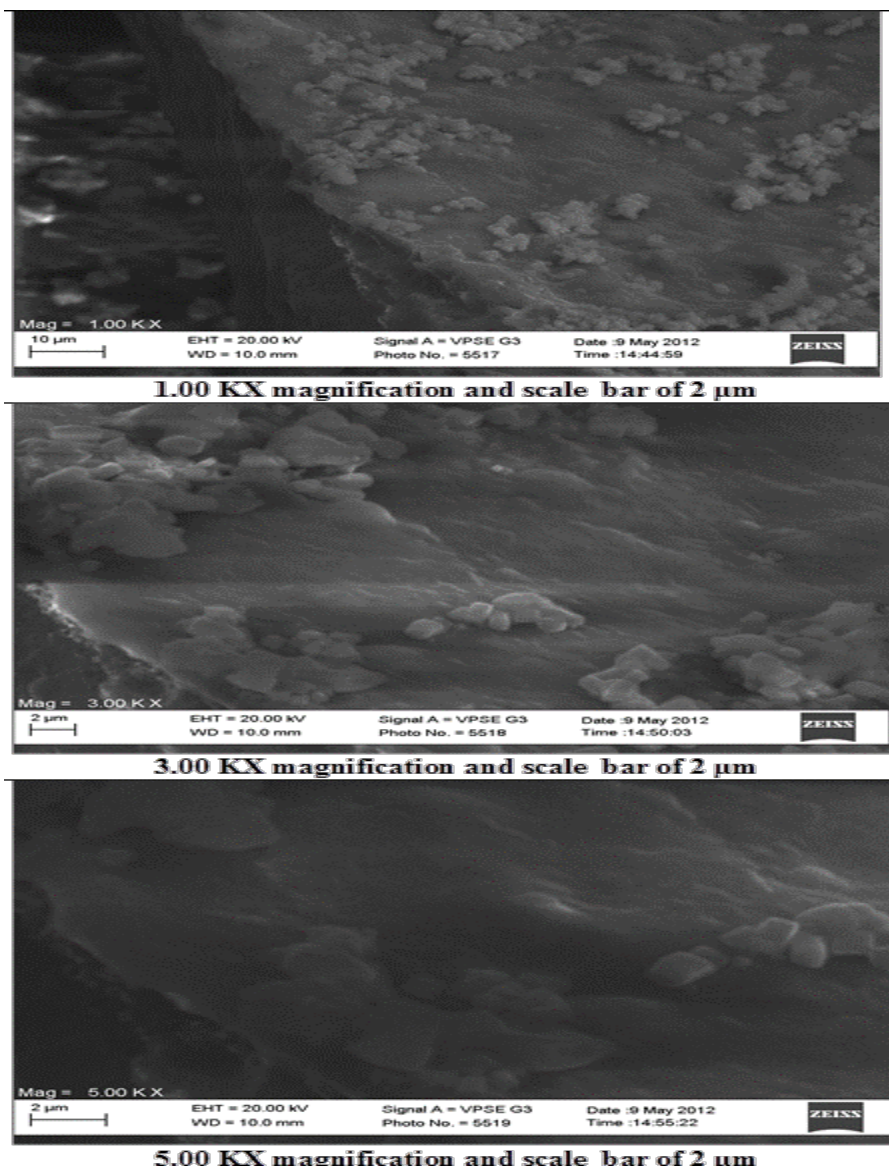Mag = 1.00 K X
10 µm   EHT = 20.00 kV   Signal A = VPSE G3   Date :9 May 2012   ZEISS
          WD = 10.0 mm   Photo No. = 5517   Time :14:44:59
1.00 KX magnification and scale bar of 2 µm

Mag = 3.00 K X
2 µm   EHT = 20.00 kV   Signal A = VPSE G3   Date :9 May 2012   ZEISS
          WD = 10.0 mm   Photo No. = 5518   Time :14:50:03
3.00 KX magnification and scale bar of 2 µm

Mag = 5.00 K X
2 µm   EHT = 20.00 kV   Signal A = VPSE G3   Date :9 May 2012   ZEISS
          WD = 10.0 mm   Photo No. = 5519   Time :14:55:22
5.00 KX magnification and scale bar of 2 um

Figure 3 Scanning electron microgram of RH gum at various magnifications.

The figures revealed that the gum consists of aggregates of irregular shapes and dimensions. Existence of molecular slaps or cavity can also be seen at the left hand side of the micrographs.

Sorption study

Figure 4 presents the variation of % moisture sorption with time for *RH* gum. The figure revealed that the percentage of moisture adsorbed by the gum increases within the first 5 days up to a maximum of 60 %. Within the sixth and seventh days, the percentage moisture sorption decreases sharply and gradually descended to a steady rate after 8 days. The pattern of plot obtained for this gum is comparable to those obtained for some other plant gums [6,21]. The plot clearly shows that the gum has strong potential to absorb moisture and due to its glucose or sugar content; it may undergo degradation if it is exposed to the air. Therefore, the gum should be stored in an air/moisture free environment.

Figure 4 Variation of % water sorption with time for *RH* gum. C is for concentration.

Rheological study
Variation of viscosity with concentration and pH

Absolute viscosity is a measure of internal resistance to shear or flow and is caused by intermolecular friction exerted when layers of fluids attempt to slide by one another. From **Figure 5**, it can be seen that the dynamic viscosity of the studied gums tend to increase with an increase in concentration.
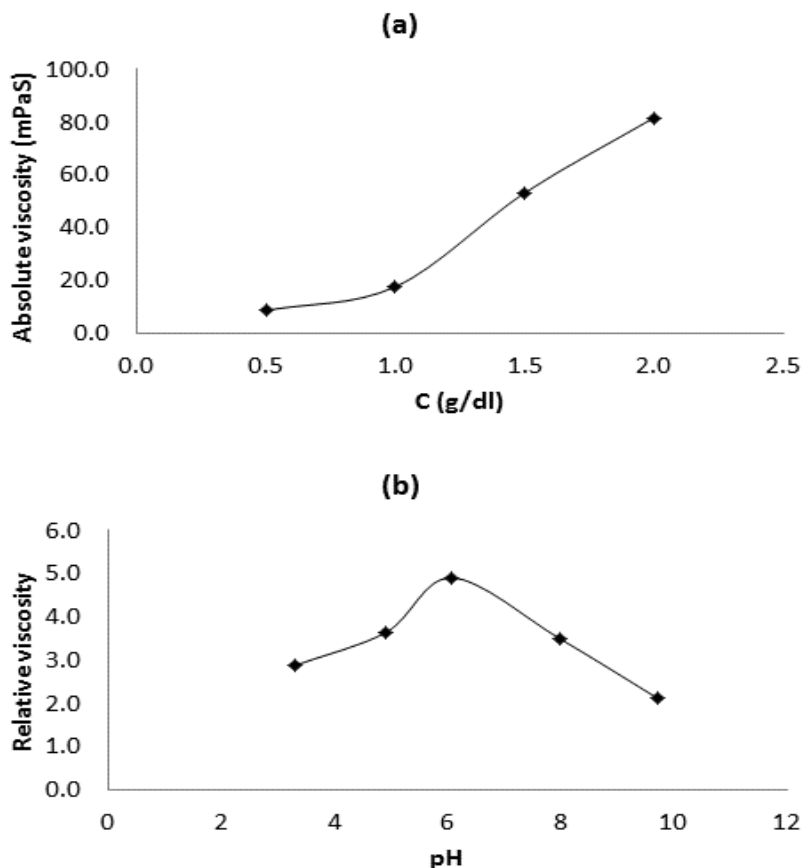
Figure 5 Variation of viscosity with (a) concentration and (b) pH of the *RH* gum. C is for concentration.

According to Newton's law of friction, dynamic or absolute viscosity of a polymer can be expressed as follows [28];

$$\eta = \tau \frac{1}{dC/dy} \tag{1}$$

where τ is the shearing stress, dC/dy is the concentration gradient. From Eq. (1), it can be seen that at constant shear rate, the absolute viscosity of a viscous fluid is expected to increase with an increase in concentration as shown in **Figure 5**. The figure also shows a plot for the variation of specific viscosity with pH for the *RH* gum. It is evident from the plot that the specific viscosity of the gum tends to increase with an increase in pH up to a pH value of about 6, after which the viscosity drops sharply, even as the pH increases. The observed trend can be explained as follows. At low pH, the electrostatic repulsions between the gum particles increases, and the particles present a decreasing association due to possible formation of hydrogen bonds, Van der Waals interactions and other weak forces. Therefore the viscosity of the gums increases until a certain critical pH is approached. Above a critical pH (pH = 6 and 8 for *RH*), the dissociation of the particles may increase due to a decrease in the strength of electrostatic repulsions. Therefore, the viscosity of the gum (*RH* gum) will decrease.

Intrinsic viscosity

Intrinsic viscosity [η] is a measure of the hydrodynamic volume occupied by a macromolecule and is closely related to the size and conformation of the macromolecular chains in a particular solvent [29,30]. Several methods are available for the determination of intrinsic viscosity of a polymer solution. These methods are based on Huggins, Kraemer and Tanglapaibul and Roa models. The Huggins model considers the relationship between intrinsic viscosity and viscosity of dilute polymer solutions in terms of a power series, which can be written as follows;

$$\frac{\eta_{sp}}{C} = [\eta] + k_1[\eta]^2 C + k_2[\eta]^3 C^2 + k_3[\eta]^4 C^3 + \dots \tag{2}$$

where [η] is the intrinsic viscosity, η_{sp} is the specific viscosity which is related to relative viscosity, η_{rel} and the reduced viscosity, η_{red}. The reduced viscosity becomes the intrinsic viscosity as C→0 and can be expressed as follows;

$$[\eta] = \lim_{c \to 0} \frac{\eta_{sp}}{C} \tag{3}$$

The power series represented by the above equation is often truncated to a linear approximation known as Huggins equation [31];

$$\frac{\eta_{sp}}{C} = [\eta] + k_H[\eta]^2 C \tag{4}$$

From Eq. (4), it can be seen that a plot of η_{sp}/C versus C will give a straight line with the slope and intercept equal to $K_H[\eta]^2$ and [η] respectively. This method of determination of intrinsic viscosity is called the graphic double extrapolation procedure. **Figure 6** shows a Huggins's plot for *RH*. Huggins parameters deduced from the plots are presented in **Table 4**.
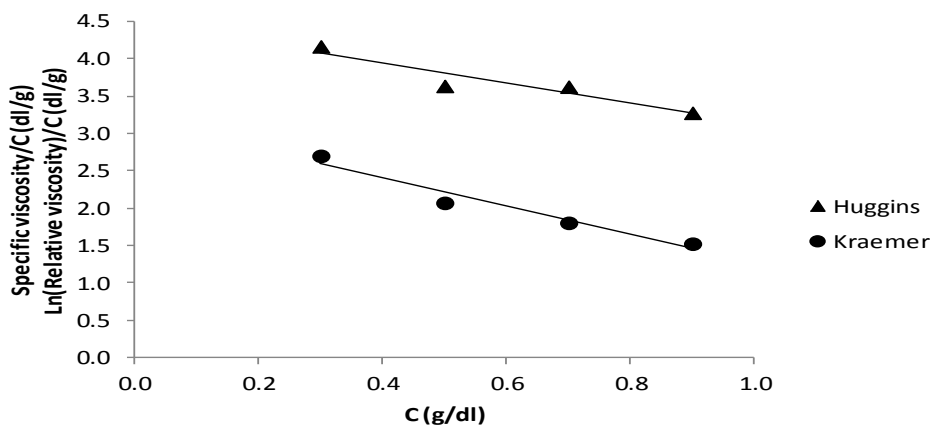

Figure 6 Huggins and Kraemer plot for *RH* gum. C is for concentration.

The results revealed that the degree of fitness of the data to Huggins's model is approximately 0.8 while the intrinsic viscosity and Huggins's constant were calculated to be equal to 4.49 and 0.1255 respectively. According to Pamies *et al.* [32], flexible polymer chains possess K_H values in the range 0.2 - 0.8. The value of K_H in this work is less than the expected minimum in the range. Pamies *et al.* [32],

related the unusual Huggins constant to solutions where the solute molecules have a tendency to associate, either by forming well defined oligomers or aggregates.

Table 4 Huggins, Kraemer, Tanglerpaibul and Roa constants for RH gum.

Model	Parameters	Magnitude
Huggins	$[\eta]$ **(g/dl)**	4.487
	R^2	0.8885
	K$_H$	0.10
Kraemer	$[\eta]$ **(g/dl)**	3.167
	R^2	0.9504
	K$_K$	0.19
Huggins/Kraemer	**K$_H$ + K$_K$**	0.30
Eq. (6)	$[\eta]$ **(g/dl)**	2.255
	Intercept	1.1305
	R^2	0.9984
Eq. (7)	$[\eta]$ **(g/dl)**	1.541
	Intercept	0.2514
	R^2	0.9902
Eq. (8)	$[\eta]$ **(g/dl)**	1.505
	Intercept	0.2645
	R^2	0.9549

The observed K$_H$ value therefore indicates heterogeneity of the solute and concentration dependence of the composition of the *RH* gum, which is frequent among biopolymers.

The intrinsic viscosity can also be determined using Kraemer's equation, written as follows [15];

$$\frac{ln\,\eta_{rel}}{C} \quad = \quad [\eta] \quad + \quad k_K[\eta]^2 C \tag{5}$$

where K$_K$ is the Kraemer constant and η_{rel} is the relative viscosity of the gum. From Eq. (5), a plot of $ln\eta_{rel}/C$ versus C is expected to be linear, provided the Kraemer equation is obeyed. The Kraemer plot for the RH gum is also presented in **Figure 6** and values of Kraemer constants are also recorded in **Table 4**. Although the value of the $[\eta]$ deduced from the Kraemer's plot (3.17) is less than the value obtained from the Huggins's plot, a better correlation (R^2 = 0.9504) is displayed in the Kraemer's plot. It has been found that the sum of K$_H$ and K$_K$ should be equal to 0.5. However, in this work, K$_H$ + K$_K$ = 0.20 indicating that there is molecular association or polymer aggregation in the studied gum [33].

Huggins and Kraemer methods of determination of intrinsic viscosity are based on extrapolation of the intercept to zero concentration. It has been found that methods of determination of intrinsic viscosity based on slopes give better correlation than those obtained from intercept methods [34]. In view of this, Tanglertpaibul and Rao [35], successfully derived the model and listed them as follows;

$$\eta_{rel} \quad = \quad 1 - [\eta]C \tag{6}$$

$$\eta_{rel} \quad = \quad exp^{[\eta]C} \tag{7}$$

$$\eta_{rel} \quad = \quad \frac{1}{1 - [\eta]C} \tag{8}$$

From Eq. (6), a plot of η_{rel} versus C should be linear and the slope should be equal to $[\eta]$. Similarly, the implication of Eq. (7) is that a plot of $\ln(\eta_{rel})$ versus lnC should be linear with slope equal to $[\eta]$ and from Eq. (8), the $[\eta]$ is a slope obtained from a plot of $1 - (1/\eta_{rel})$ versus C. **Figure 7** shows Tanglerpaibul and Roa plots according to Eqs. (6) - (8) respectively.
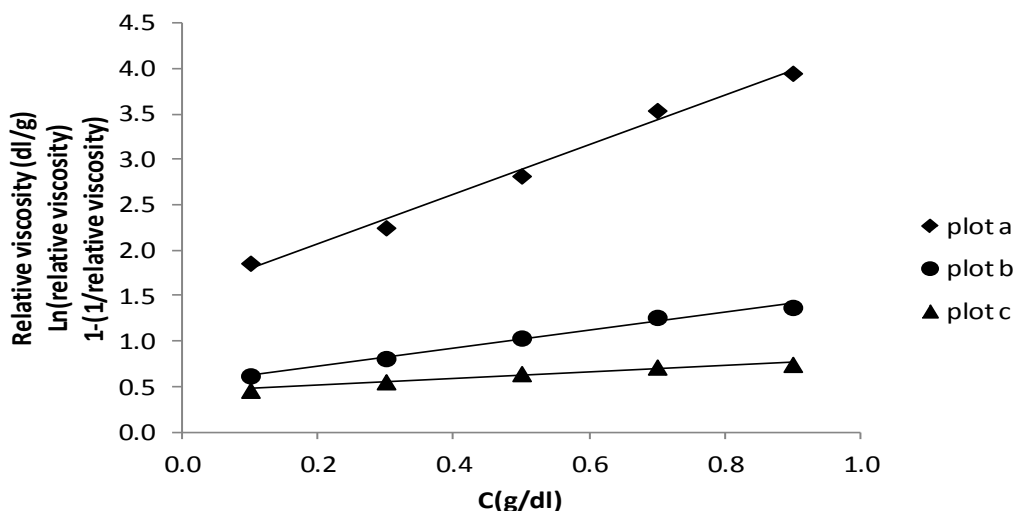

Figure 7 Variation of η_{rel} (plot a), $\ln(\eta_{rel})$ (plot b) and $1 - (1/(\eta_{rel})$(plot c) with C for RH gum. C is for concentration.

Calculated values of $[\eta]$ obtained from the slopes of the plots are presented in **Table 4**. From the results obtained, it can be seen that better correlation coefficients are obtained from the plots. However, calculated values of intrinsic viscosity are approximately equal to 2.0, which differ from those obtained from the Huggins and Kraemer model. Similar observation was found by Higiro *et al*. [4] for xanthan and locust bean gums.

Coil-overlap parameter and molecular conformation

Coil overlap and interpenetration is typical for a concentrated solution as distinct from a dilute solution, where the individual molecules are free to move independently. Chou and Kokoni [34] found that the transition from dilute to concentrated solution is usually accompanied by a pronounced change in the concentration dependence of solution viscosity and that the corresponding concentration is called critical or coil overlap concentration. The coil overlap parameter can be studied using a double logarithm plot of η_{sp} against $C*[\eta]$. **Figure 8** shows the master curve for *RH* gum. The linearity of the plot suggests the existence of a dilute Newtonian domain in the *RH* gum. The slope of the plot was 0.8 which is close to the 0.9 reported by Higiro *et al*. [4] for xanthan and locust bean gums and to the value of 1.4 reported for most food gums by Morris *et al*. [36]. In this study, there was no change in the slope of the master plot for the *RH* gum, within the studied concentration indicating that there is no molecular entanglement.
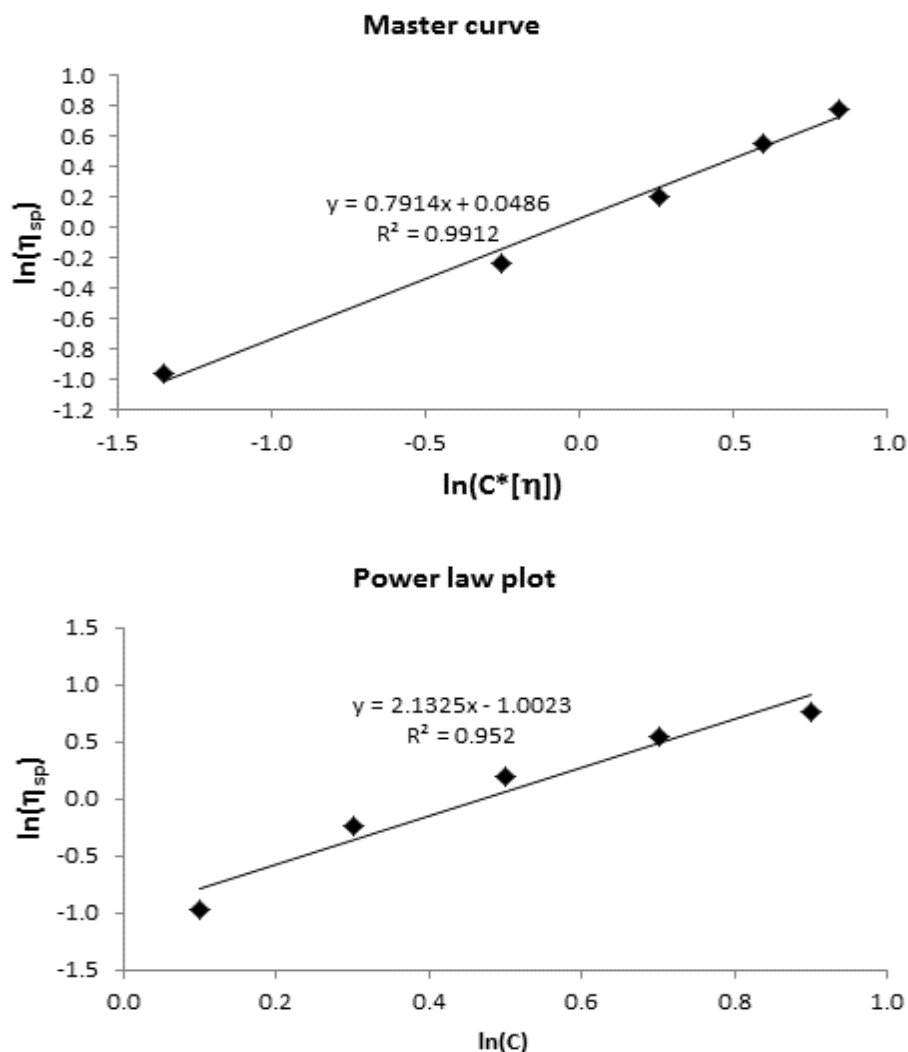
Figure 8 Master and Power law plots for the *RH* gum. C is for concentration.

The power law model (Eq. 9) was used to study molecular conformation for the *RH* gum exudates [4];

$$\eta_{sp} = aC^b \tag{9}$$

The constants 'a' and 'b' are indicators for conformation of a polysaccharide. They can be estimated by plotting values of log (η_{sp}) versus *log* (C). The Power law plot for *RH* gum is also shown in **Figure 8**. From the plot, the slope value (2.1) was found to be greater than unity. In dilute regimes, slope values greater than unity have been reported to be associated with random coil conformation [37] or entanglement [36]. This finding agrees with the information revealed in the scanning electron micrograph of the gum (**Figure 3**), in which the gum is seen to present a random coil conformation.

Effect of temperature

Figure 9 shows a plot for the variation of viscosity of *RH* gum with temperature. A decrease in viscosity was observed for the gum solution at a concentration of 2 g/dl. The absence of degradation or conformational transition was indicative due to similarity in graphs during heating and cooling.
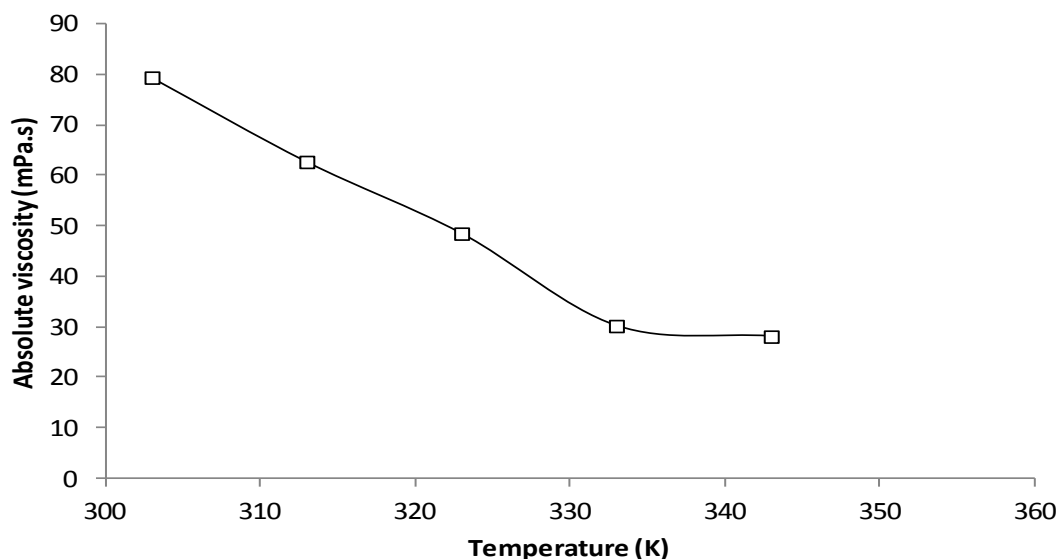

Figure 9 Variation of absolute viscosity of the *RH* gum with temperature.

The absence of a conformational transition was also studied using the Arrhenius-Frenkel-Eyring equation, Eq. (10) [38];

$$\eta \quad = \quad A exp \left(\frac{E_F}{RT} \right) \tag{10}$$

where A is the pre-exponential factor, E_F is the activation energy of flow, R is the universal gas constant and T is the absolute temperature in Kelvin. Simplification of Eq. (10) yields Eq. (11);

$$\ln \eta \quad = \quad lnA \quad + \quad \frac{E_F}{RT} \tag{11}$$

Eq. (11) revealed that a plot of lnη versus 1/T should be linear with a slope and intercept equal to E_F and lnA respectively. **Figure 10** shows the Arrhenius-Frenkel-Eyring plots for *RH* gum exudates. The apparent activation energy Activation parameters deduced from the plots are presented in **Table 5**.
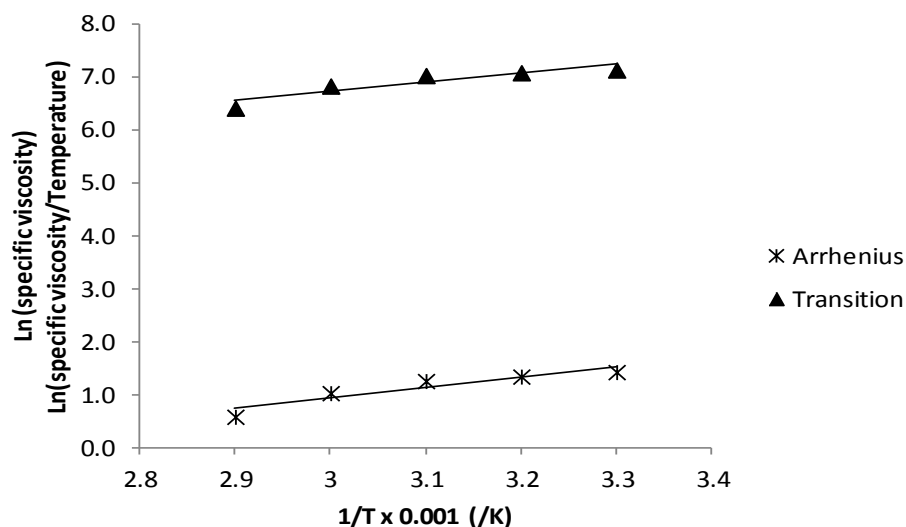
Figure 10 Variation of ln(η)/ln(η/T) with 1/T for *RH* gum.

Table 5 Thermodynamic parameters of viscous flow for *RH* gum.

Transition state		Arrhenius	
Slope	2.808	**Slope**	2.808
ΔH_v (kJ/mol)	23.35	**E_F (J/mol)**	23.35
A	0.0076	**lnA**	−4.8771
ΔS_v (kJ/mol)	−0.7069	**A**	0.007619
R²	0.9655	**R²**	0.9655

The apparent activation energy of flow (23.35 kJ/mol) obtained from the slope of the plot is comparable to those obtained for 2 % solution of *Albezia lebbeck* gum (16.6 kJ/mol) [14], Arabic gum (15 kJ/mol) [39] and that of *A. occidentale* gum (16.2 kJ/mol) [40]. Generally, low activation energy of flow indicates few inter- and intractions between the polysaccharide chains in the concentration range investigated. *RH* gum therefore, has the tendency to exhibit strong intra- and intermolecular interactions since its E_F value is comparable to those of linear polymers that exhibit such characteristics. For example, E_F value for 4 % carboxylmethyl cellulose is reported to be 27 kJ/mol [14].

According to Acevedo and Katz [28], thermodynamic parameters of viscous flow can be calculated using the Frenkel-Eyring equation in the form;

$$ln\left(\frac{\eta}{T}\right) \;=\; \left(ln\left(\frac{R}{Nh}\right) \;-\; \frac{\Delta S_V}{R}\right) \;+\; \frac{\Delta H_V}{RT} \tag{12}$$

where N is Avogadro's number and h is the Plank constant, T is the absolute temperature, ΔS_V and ΔH_V are the changes in entropy and enthalpy of viscous flow. From Eq. (12), a plot of ln(η/T) versus 1/T is expected to be linear with slope and intercept equal to $\frac{\Delta H_V}{R}$ and (ln(R/Nh) − ΔS_V/R) respectively. The Transition state plot for *RH* gum and the thermodynamic parameters deduced from the plot are shown in

Figure 10 and **Table 5** respectively. Calculated values of ΔH_V were found to be positive while those of ΔS_V were negative indicating that the attainment of the transition state for viscous flow is accompanied by bond breaking. According to Sannin [41] negative values of ΔS_V is associated with uncoiling and orientation of the polymer molecules and the system becomes more ordered in the course of flow while positive values of ΔH_V is related to the amount of energy needed by the gum molecules to jump from one equilibrium position to another (i.e. the potential energy barrier).

Effect of electrolyte

Exudates gums are acid polysaccharides and therefore behave as polyelectrolyte indicating that the solution viscosity of the gums can be affected by the addition of other electrolytes [14]. In this study, the effects of KCl, CaCl$_2$, AlCl$_3$ and urea on the viscosity of *RH* gum were investigated. **Figure 11a** shows the variation of viscosity of *RH* gum with concentrations in the presence of 0.1 M KCl, CaCl$_2$, AlCl$_3$ and urea.
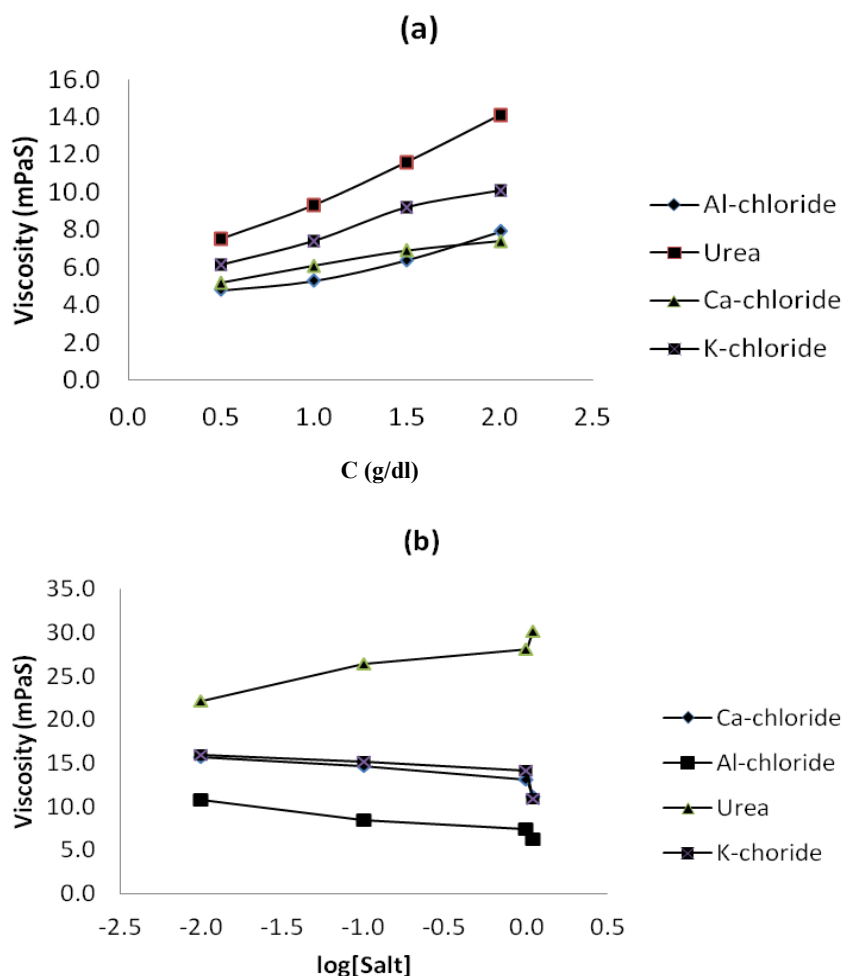

Figure 11 Variation of viscosity with (a) concentration of RH gum in the presence of 0.1 M of various electrolytes (KCl, CaCl$_2$, AlCl$_3$ and urea), (b) various concentration of K$^+$, Ca^{2+}, Al^{3+} and urea at 298 K.

The viscosity of the *RH* gum seems to be raised by the presence of urea while KCl, CaCl$_2$ and AlCl$_3$ decreased the viscosity of the gum in accordance with their ionic charge (i.e. Al^{3+} > Ca^{2+} > K$^+$). According to de Paula *et al.* [14], the decrease in viscosity through addition of electrolyte can be attributed to existence of fewer intermolecular interactions due to the screening charges and contraction of the macromolecule in the presence of a counter ion. Aluminum has a tendency to establishing strong interactions with macromolecules through intermolecular cross linking effects. On the other hand, the strength of the intermolecular cross linking effect is lower in Ca^{2+} than in aluminum while sodium is not a cross linking agent. This explains the order observed for the decrease in viscosity of the gum. It is also significant to note that the affinity of the studied gum for counter ions depends on the charge/ionic ratio. Generally, ions with higher charge will have a stronger affinity for the molecular chain of the gum. The charge to ionic radius ratio of K$^+$, Ca^{2+} and Al^{3+} are 0.66, 1.75 and 4.41 respectively hence the expected order for the interaction of the studied gums with metal ions is Al^{3+} > Ca^{2+} > K$^+$, which is in agreement with the findings of this study.

Urea significantly increases the viscosity of the gum solution due to its tendency to form a porous framework. Urea has the ability to trap many organic compounds. In its so-called clathrates, the organic "guest" molecules are held in channels formed by interpenetrating helices composed of hydrogen-bonded urea molecules.

Ionic strength can affect the thickness of the electrical double layer around the charged interfaces as well as modifying the conformation of the polymer attached to the surface (i.e. spatial extension). In order to study the effect of ionic strength on the viscosity of *RH* gum, apparent viscosity of 1 % (w/v) solution of the gum (containing various concentrations of K$^+$, Ca^{2+}, Al^{3+} and urea) were measured. **Figure 11b** shows the variation of apparent viscosity of 1 % solution of *RH* gum with concentrations of electrolytes (K$^+$, Ca^{2+}, Al^{3+} and urea). The plots revealed that the apparent viscosities of the gum decreases with increase in the logarithm of the salt concentration indicating the contribution of the shielding and cross linking effect. The cross linking effect seems to be more prevalent in the presence of Al^{3+}. In the presence of Ca^{2+} contribution of screening effect leads to chain contraction. In K$^+$, the shielding effect dominates and the chain contracts leading to an elevated chain contraction. As stated earlier, shielding and cross linking effect is associated with the ratio of charge to ionic charge of the metal. In Al^{3+}, the ratio is highest therefore cross linking effect dominates but K$^+$ having the least ratio displayed strong shielding effect. Sanin [41], had found that an increase in the ionic strength of a polymer solution will lead to a decrease in viscosity because as more ions are added to the system, the viscosity starts to give less respond, changing minimally. In this case, the electrical double layer is compressed at high ionic strengths, particles and flocs may assume closer localities with each other and the surface polymer may also assume a coiled conformation rather than a stretch conformation.

Steady shear properties

Based on the variation of viscosity with shear rate, or shear stress with shear rate, the polymer solution can be classified as Newtonian or non Newtonian. Newtonian fluids are fluids which have a constant viscosity indicating that a plot of shear stress versus shear rate for Newtonian fluid should be linear, passing through the origin [13,15]. Plots for the variation of shear stress with shear rate for the *RH* gum (plot not shown) revealed that the gum is non Newtonian and displayed pseudo-plastic flow behavior, characterized by thinning. According to Ameh *et al.* [33], Newtonian and non Newtonian behavior of gums can also be investigated by plotting speed of rotation versus corresponding viscosity. If such plots are linear, then a non Newtonian behavior is upheld. Plot of viscosity versus speed of rotation for *RH* gum also revealed that *RH* gum is a non-Newtonian fluid.

In pseudo-plastic non Newtonian flow phenomenon, viscosity decreases with shear rate because both secondary and primary bonds are being broken isothermally and reversibly [16]. Clusters and aggregates of particles originally present in the suspension are destroyed by shear. Specific mechanisms responsible for this kind of rheological behavior are:

(i) Structure-breaking due to hydrodynamic effects where the rate of particle disassociation is greater than the rate of their association.

(ii) Favorable orientation of macromolecules or dispersed asymmetric particles in the flow field.

(iii) Diminution or removal of the absorbed film (solvation layer) surrounding the particles due to hydrodynamic effects.

The degree of shear-thinning depends on the structural state of the dispersion prior to shearing and on the composition of the dispersing phase. Consequently, hydrocolloids are excellent shear-thinning agents.

Conclusions

RH gum is rich in essential chemicals, nutrients, major and trace elements. The gum has low concentrations of anti-nutrients and toxic heavy metals. The gum possesses unique properties that can enhance its utilization as an emulsifying agent and pharmaceutical excipient. The gum seems to function effectively in a non Newtonian domain and is not responsive to conformational degradation but exhibits flow properties that are consistent with the existence of strong intra- and intermolecular bonds. Theoretical modeling and surface morphology of the gums agree on the existence of random like nature and molecular association between the molecules. Functional groups identified in the gum are typical to those found in polysaccharides.

References

[1]   UD Akpabio, AE Akpakpan, UE Udo and UC Essien. Physicochemical characterization of exudates from Raffia Palm. *Adv. Appl. Sci. Res*. 2012; **3**, 838-43.

[2]   A Berner-Strzelczyk, J Kolodziejska and MM Zgoda. Application of guar gum biopolymer in the prescription of tablets with sodium ibuprofen-quality tests and pharmaceutical availability *in vitro*. *Polim. Med*. 2006; **36**, 3-11.

[3]   PO Ameh and NO Eddy. *Commiphorapedunculata* gum as a green inhibitor for the corrosion of aluminium alloy in 0.1 M HCl. *Res. Chem. Intermed.* 2014; **40**, 2641-9.

[4]   J Higiro, TJ Herald and S Alavi. Rheological study of xanthan and locust bean gum interaction in dilute solution. *Food Res. Int.* 2006; **39**, 165-75.

[5]   DE Okwu and FU Nnamdi. Evaluation of the chemical composition of *Dacroydes edulis* and *Raphia hookeri mann and wendi* exudates used in herbal medicine in South Easth Nigeria. *Afr. J. Tradit. Complement. Altern. Med*. 2008; **5**, 194-200.

[6]   NO Eddy, PO Ameh, CE Gimba and EE Ebenso. Rheological modeling, surface morphology and physicochemical properties of *Anogeissusleiocarpus g*um. *Asian J. Chem.* 2013; **25**, 1666-72.

[7]   GS Mhinzi. Properties of gum exudates from selected *Albizia* species from Tanzania. *Food Chem.* 2002; **77**, 301-4.

[8]   OHM Idris, PA Williams and GO Phillips. Characterization of gum from *Acacia senegal* trees of different age and location using multidetection gel permeation chromatography. *Food Hydrocolloid.* 1998; **12**, 379-88.

[9]   JK Lelon, IO Jumba, JK Keter, W Chemuku and FDO Oduor. Assessment of physical properties of gum arabic from Acacia Senegal varieties in Baringo District, Kenya. *Afr. J. Phys. Sci.* 2010; **4**, 95-8.

[10] JS Alakall, SV Irtwange and M Mkavga. Rheological characteristics of food gum (Cissuspopulnea). *Afr. J. Food Sci.* 2009; **3**, 237-42.

[11] MM Jafar, E Zahra, S Mohammad, M Mohammad and G Babak. Physicochemical and emulsifying properties of Barijeh (Ferula gumosa) gum. *Iran. J. Chem. Chem. Eng.* 2007; **26**, 81-8.

[12] SE Ahmed, BE Mohamed and KA Karamalla. Analytical studies on the gum exudates from *Anogeissuslei carpus. Pakistan J. Nutr.* 2009; **8**, 782-8.

[13] EI Yassen, TJ Herald, FM Aramouni and S Alavi. Rheological properties of selected gum solutions. *Food Res. Int.* 2005; **38**, 111-9.

[14] RCM de Paula, SA Santana and JF Rodrigues. Composition and rheological properties of *Albizia lebbeck* gum exudate. *Carbohydr. Polym*. 2001; **44**, 133-9.

[15] K Khounvilay and W Sittikijypthin. Rheological behavior of tamarind seed gum in aqueous solutions. *Food Hydrocolloid.* 2012; **26**, 334-8.

[16] FF Simas-Tosin, RR Barraza, CLO Petkowicz, JLM Silveira, GL Sassaki, EMR Santos, PAJ Gorin and M Iacomini. Rheological and structural characteristics of peach tree gum exudates. *Food Hydrocolloid.* 2010; **24**, 486-93.

[17] X Ma and M Pawlik. Adsorption of guar gum onto quartz from dilute mixed electrolyte solutions. *J. Colloid Interface Sci.* 2006; **298**, 609-14.

[18] BA Ndon. Some morphological and chemical characteristics of developing fruits of *Raphia hookeri J. Exp. Botany* 1985; **36**, 1817-30.

[19] Association of Official Analytical Chemists. *Official Methods of Analysis.* 13th ed. Horwitz, Benjamin Franklin Station, Washington DC, 1995.

[20] HG Muller and G Tobin. *Nutrition and Food Processing.* Croom Helm, London, 1980.

[21] NO Eddy, I Udofia, A Uzairu and C Obadimu. Physicochemical, spectroscopic and Rheological studies on *Eucalyptus Citrodora* (*EC*) gum. *J. Polym. Biopolym. Phys. Chem.* 2014; **2**, 12-24.

[22] MP Yadav, N Parris, DB Johnson and KB Hicks. Fractionation, characterization, and study of the emulsifying properties of corn fibre gum. *J. Agric. Food Chem.* 2008; **56**, 4181-7.

[23] KA Karamalla, NE Siddig and ME Osman. Analytical data for *Acasia Senegal var, Senegal* gum samples collected between 1993 and 1995 from Sudan. *Food Hydrocolloid.* 1998; **12**, 373-8.

[24] DE Okwu and OD Omodamiro. Effect of Hexane extract and phytochemical content of Xylopia aethiopica and Ocimum gratissimum on uterus of Guinea pig. *BioResearch* 2005; **3**, 40-4.

[25] VTP Vinod and RB Sashidhar. Surface morphology, chemical and structural assignment of gum Kondagogu (Cochlospermum gossypium DC): An exudates tree gum in India. *Ind. J. Nat. Prod. Res.* 2010; **1**, 181-92.

[26] M Xiaodong and P Marek. Intrinsic viscosities and Huggins constants of Guar gum in alkali metal chloride solutions. *Carbohydr. Chem.* 2007; **10**, 15-24.

[27] DK Setua, R Awasthi, S Kumar, M Prasad and K Agarwal. *Scanning Electron Microscopy of Natural Rubber Surfaces: Quantitative Statistical and Spectral Texture Analysis using Digital Image Processing. In*: A Méndez-Vilas and J Díaz (eds.). Microscopy: Science, Technology, Applications and Education, Formatex, Spain, 2010

[28] IL Acevedo and M Katz. Viscosities and thermodynamics of viscous flow of some binary mixtures at different temperatures. *J. Solution Chem.* 1990; **19**, 1041-52.

[29] S Al-Assaf, GO Phillips and PA Williams. Studies on Acacia exudates gums: part II, Molecular weight comparison of the Vulgares and Gummiferae series of Acacia gums. *Food Hydrocolloid.* 2005; **19**, 661-7.

[30] J Higiro, TJ Herals, S Alvi and S Bean. Rheological study of xanthan and locust bean gum interaction in dilute solution: Effect of salt. *Food Res. Int.* 2007; **49**: 435-47.

[31] ML Huggins. The viscosity of dilute solution of long chain molecules IV. Dependence on concentration. *J. Am. Chem. Soc.* 1942; **64**, 2716-8.

[32] K Pamies, JGH Cifre, MC Martinez and JG de la Torre. Determination of intrinsic viscosities of macromolecules and nanoparticles. Comparison of single-point and dilution procedures. *Colloid Polym. Sci.* 2008; **286**, 1223-31.

[33] PO Ameh, NO Eddy and CE Gimba. *Physiochemical and Rheological Studies on Some Natural Polymers and Their Potentials as Corrosion Inhibitors.* Lambert Academic Publishing, UK, 2012.

[34] TD Chou and JL Kokini. Rheological properties and conformation of tomato paste pectins, citrus and apple pectins. *J. Food Sci.* 1987; **52**, 1658-64.

[35] T Taglertpaibul and MA Rao. Intrinsic viscosity of tomato serum as affected by methods of determination and methods of processing concentrates. *J. Food Sci.* 1987; **32**, 1642-88.

[36] ER Morris, AN Cutler, SB Ross-Murphy, DA Ress and J Price. Concentration and shear rate dependence of viscosity in random coil polysaccharide solutions. *Carbohydr. Polym.* 1981; **1**, 5-21.

[37] R Lapasin and S Pricl. *Rheology of Polysaccharide Systems. In*: R Lapasin and S Pricl (eds.). Rheology of industrial polysaccharides: Theory and applications Blackie Academic and Professional, Glasgow, 1995, p. 250-494.

[38] AS Eissa. Newtonian viscosity behavior of dilute solutions of polymerized whey proteins. Would viscosity measurements reveal more detail molecular properties? *Food Hydrocolloid.* 2013; **30**, 200-5.

[39] EP Varfolomeeva, VY Grinberg and VB Toistogusov. Rheology of polymer. *Polym. Bull.* 1980; **2**, 613-8.

[40] AG Silva, JF Rodrigues and RCM de Paula. Composição e propriedades reológicas da goma do angico (Anadenanthera Macrocarpa Benth). *Polimeros* 1998; **4**, 34-40.

[41] FD Sanin. Effect of solution physical chemistry on the rheological properties of activated sludge. *Water SA* 2002; **28**, 207-12.

[42] S Asokan, KM Krueger, A Alkhawaldeh, AR Carreon, Z Mu, VL Colvin, NV Mantzaris and MS Wong. The use of heat transfer fluids in the synthesis of high-quality CdSe quantum dots, core/shell quantum dots, and quantum rods. *Nanotechnology* 2005; **16**, 2000-11.

[43] S Yageswari, S Ramakakshmi, R Neelavathy and J Muthumary. Identification and comparative studies studied of different volatile fractions from Monochaetia kansensis by GCMS. *Global J. Pharmacol.* 2012; **6**, 65-71.

[44] GL Darmstadt, M Mao-Qiang, E Chi, SK Saha, VA Ziboh, RE Black, M Santosham and PM Elias. Impact of topical oils on the skin barrier: possible implications for neonatal health in developing countries. *Acta Paediatr.* 2002; **91**, 546-54.

Appendix

Some industrial applications of compounds in *RH* gum.

Line no	IUPAC name	Industrial application
1	1-undecene	Use as fuel and an industrial chemical
2	3-hexadecene	Use as a shorthand for cetane number, a measure of the detonation of diesel fuel
3	3,5-di-tert-butylphenol	Use industrially as UV stabilizer and an antioxidant for hydrocarbon-based products ranging from petrochemicals to plastics [42]
4 5	3-octadecene 1-butylheptyl benzene	Octadecene is used in the synthesis of colloidal quantum dot
6	1-propyloctyl benzene	Commonly use as plasticizer; as an additive to adhesives or printing inks and as an ectoparasiticide
7	1-butyloctyl bezene	Use in the manufacture of specialty paper
8	1-Docosene	Component of oil field chemicals, wax replacement and as lube oil additives [43]
9	Palmitic acid	In the production of soap, cosmetics and as a release agent
10	n-hexadecanoic acid	Use as a lubricant and as an additive in industrial preparations
11	9,12-octadecadienoic acid	
12	10-octadecenoic acid	Use as a surfactant and in cosmetic formulation [44]
13	n-octadecanoic acid	
14	Nonanenitrile	Use in the textile industries